

C

arolina

Nov

12&13

20

S

cience

S

ymposium



Online

Cover photo is Lakeside by Jon Meyer 2019 Mike Rigsbee Memorial Photo Contest Winner

## Contents

ORGANIZING COMMITTEE .....	5
FRED STEVIE .....	5
DR. JOHN LANNON, JR .....	5
JOE BECKER .....	5
DR. CHARLES PARKER .....	5
ROBERTO GARCIA .....	5
DR. BOB GEIL.....	5
DR. PHILIP BARLETTA.....	6
DR. SHANTHI IYER.....	6
TOBY TUNG.....	6
ANDY NEWELL.....	6
DR. MAUDE CUCHIARA .....	6
PHILLIP STRADER.....	6
DR. DANIEL HERR.....	6
CHUCK MOONEY .....	6
ANNA LUMPKIN.....	6
AWARDS .....	7
AGENDA NOV 12.....	8
AGENDA NOV 13.....	9
NOV 12 SPEAKERS.....	10
BIOLOGICAL MICRODEVICES .....	10
ROGER NARAYAN .....	10
PATTERNING HYBRID PEROVSKITE SINGLE CRYSTALS BY SURFACE-ENGINEERED DELIQUESCENT AND EFFLORESCENCE.....	11
JONATHAN K. MEYERS, LORENZO Y. SERAFIN, ANDRE ORR, AND JAMES F. CAHOON .....	11
DETERMINISTIC DESIGN OF ENERGY STORAGE ELECTRODES THROUGH OXIDE ELECTRODEPOSITION IN CNT FOAM SCAFFOLDS .....	12
ISHITA KAMBOJ (1), MICHAEL SPENCER (1), OZKAN YILDIZ (2), PHILIP D. BRADFORD (2), & VERONICA AUGUSTYN (1) .....	12
UNEXPECTEDLY LARGE REMANENT POLARIZATION IN FERROELECTRIC Hf <sub>0.5</sub> Zr <sub>0.5</sub> O <sub>2</sub> CAPACITOR ON 002 TEXTURED TiN.....	13
YOUNGHWAN LEE, H. ALEX HSAIN, GREGORY PARSONS, JACOB L. JONES .....	13
CONTROL OF FIBER TEXTURE IN FERROELECTRIC (Hf, Zr)O <sub>2</sub> THIN FILMS USING Al <sub>2</sub> O <sub>3</sub> AND TiO <sub>2</sub> INTERLAYERS .....	14
H. ALEX HSAIN, YOUNGHWAN LEE, GREG PARSONS, JACOB JONES.....	14
A STUDY OF N-DOPING IN MBE GROWN GaAsSb NANOWIRES USING GaTe DOPANT SOURCE AND ENSEMBLE NANOWIRE NEAR-INFRARED PHOTODETECTOR.....	15
SHISIR DEVKOTA, MEHUL PARAKH, SEAN JOHNSON, PRIYANKA RAMASWAMY, MICHAEL LOWE, AUBREY PENN, LEW REYNOLDS, AND SHANTHI IYER.....	15
DILUTE NITRIDE Te-DOPED GaAsSbN NANOWIRE GROWTH AND ENSEMBLE PHOTODETECTOR APPLICATION. .....	16

RABIN POKHAREL, PRIYANKA RAMASWAMY, SHISIR DEVKOTA, MEHUL PARAKH, KENDALL DAWKINS, AUBREY PENN, MATTHEW CABRAL, LEWIS REYNOLDS, AND SHANTHI IYER .....	16
FIBER CROSS-SECTIONAL SHAPE INFLUENCES THE CELLULAR RESPONSE OF SURFACE TREATED BIODEGRADABLE BIPHASIC TISSUE ENGINEERING SCAFFOLDS FOR TENDON-BONE JUNCTION REPAIR.....	17
MARTIN W. KING AND HARSHINI RAMAKRISHNA.....	17
HYPERSPECTRAL IMAGE ANALYSIS OF GRAPHENE DERIVATIVES USING TIP-ENHANCED RAMAN SPECTROSCOPY .....	18
CHIUNG-WEI HUANG, XIAO YOU, KIZHANIPURAM VINODGOPAL, AND JOANNA M. ATKIN .....	18
AN IDEAL STRUCTURE FOR LI-ION BATTERY SEPARATORS .....	18
SALVATORE LUISO, AUSTIN WILLIAMS, ORLIN VELEV, BEHNAM POURDEYHIMI, PETER FEDKIW .....	19
GAASb/GAAs SEPARATE ABSORPTION AND MULTIPLICATION NANOWIRE AVALANCHE PHOTODIODES FOR NEAR-INFRARED PHOTODETECTION. ....	20
MEHUL PARAKH, RABIN POKHAREL, PRIYANKA RAMASWAMY, HIRANDEEP KUCHOOR, JIA LI AND SHANTHI IYER .....	20
CELLULAR AND MOLECULAR CREDENTIALING OF BREAST TUMOR HER2 STATUS USING A CELLPHONE. ....	21
SIMONE A. WALL, JACOB T. HEGGESTAD, DANIEL Y. JOH, SHENGWEI ZHANG, E. SHELLEY HWANG, KYLE C. STRICKLAND, QINGSHAN WEI, ASHUTOSH CHILKOTI .....	21
ETHANE TO LIQUIDS VIA A CHEMICAL LOOPING APPROACH – REDOX CATALYST DEMONSTRATION AND PROCESS ANALYSIS.....	22
LEO BRODY*, LUKE NEAL*, VASUDEV HARIBAL, AND FANXING LI.....	22
NOV 13 SPEAKERS.....	23
VERSATILE PEROVSKITE SEMICONDUCTORS.....	23
DAVID B. MITZI <sup>1,2</sup> .....	23
ACHIEVING NET ZERO ENERGY GREENHOUSES BY INTEGRATING SEMITRANSSPARENT ORGANIC SOLAR CELLS .....	24
ESHWAR RAVISHANKAR, RONALD E. BOOTH, CAROLE SARAVITZ, HEIKE SEDEROFF, HARALD W. ADE, AND BRENDAN T. O'CONNOR.....	24
ADDITIVE MANUFACTURING OF MINIATURIZED RFID TAG USING ELECTROCERAMIC MATERIALS FOR HIGH TEMPERATURE WIRELESS SENSING APPLICATIONS .....	25
KAVIN SIVANERI VARADHARAJAN IDHAIAM, DOMENIC CIPOLLONE, EDWARD M. SABOLSKY, KONSTANTINOS SIERROS , DARYL REYNOLDS .....	25
RECENT DEVELOPMENTS IN PYPROCAR: A PYTHON LIBRARY FOR ELECTRONIC STRUCTURE PRE/POST-PROCESSING .....	26
UTHPALA HERATH, PEDRAM TAVADZE, HE XU, ERIC BOUSQUET, SOBHIT SINGH, REESE BOUCHER, LOGAN LANG, FREDDY FARAH, FRANCISCO MUÑOZ, ALDO H. ROMERO .....	26
SILICATE MINERALS PROVIDE NON-BIOLOGICAL REMOVAL OF AMMONIUM AND PHOSPHATE IONS FROM ONSITE-WASTEWATER-TREATMENT-SYSTEM EFFLUENT .....	27
VASQUEZ, MARIANA; HAWKINS, BRIAN T.; TROTOCHAUD, LENA.....	27
SYMMETRY-BREAKING IN MICROSCALE TURBULENT POROUS MEDIA FLOW.....	28
VISHAL SRIKANTH, CHING-WEI HUANG, TIMOTHY S. SU, ANDREY V. KUZNETSOV .....	28
GROWTH AND CHARACTERIZATION OF DEVICE QUALITY INxGA1-xN TEMPLATES TO ADDRESS DROOP AND RED EMISSION IN LEDs.....	29
EVYN LEE ROUTH, MOSTAFA ABDELHAMID, N.A. EL-MASRY, S.M. BEDAIR.....	29
EMERGING WIDE BANDGAP SEMICONDUCTOR MATERIALS.....	30
HEATHER SPLAWN, KYMA.....	30

DAMAGE DETECTION IN MOISTURE CONTAMINATED POLYMER COMPOSITES THROUGH UNSUPERVISED MACHINE LEARNING .....	31
RISHABH D GUHA, KATHERINE BERKOWITZ, OGHENEVO IDOLOR, DR. LONDON GRACE .....	31
TOWARDS EFFICIENT DESIGNING OF DNA ORIGAMI NANOSTRUCTURES .....	32
JORGE GUERRERO, REZA ZADEGAN .....	32
POSTERS.....	33
ELECTRICAL AND SURFACE ANALYSIS OF MBE GROWN INTRINSIC AND TE-DOPED GAASB NANOWIRES.....	33
PRIYANKA RAMASWAMY, SHISIR DEVKOTA, RABIN POKHAREL, SURYA NALAMATI, KEITH JONES, JIA LI, AND SHANTHI IYER. ....	34
ENHANCING THE SPATIAL RESOLUTION OF NANO BEAM ELECTRON DIFFRACTION PHASE MAPPING.....	35
TIM B. ELDRED, JACOB G. SMITH, WENPEI GAO .....	35
WORK FUNCTION MODULATION IN 2D MOS <sub>2</sub> .....	36
S. POURIANEJAD, J. AVERITT, T. IGNATOVA.....	36
ADVANCED STRAIN ANALYSIS OF GRAPHENE ON IN VAN DER WAALS HETEROSTRUCTURES .....	37
KIRBY SCHMIDT, SAJEDEH POURIANEJAD, ANTHONY TROFE, TETYANA IGNATOVA .....	37
DEFORMATION OF PRUSSIAN BLUE DURING ELECTROCHEMICAL CATION INSERTION FROM AQUEOUS ELECTROLYTES .....	38
SAEED SAEED, SHELBY BOYD, WAN-YU TSAI, RUOCUN WANG, NINA BALKE, AND VERONICA AUGUSTYN .....	38
A SIMULATION STUDY OF CARRIER INDUCED CHANGE IN REFRACTIVE INDEX FOR OPTIMAL LIGHT ABSORPTION IN GAASB NANOWIRES.....	39
KENDALL DAWKINS .....	39
GREENER SYNTHESIS OF HIGH ASPECT RATIO COPPER OXIDE NANOWIRES FOR POTENTIAL APPLICATIONS.....	40
GAYANI PATHIRAJA, HEMALI RATHNAYAKE .....	40
PITCH-DEPENDENT STUDY OF PATTERNED GAASBN NANOWIRES USING BOLTZMANN SIGMOIDAL MODEL .....	41
SEAN JOHNSON, RABIN POKHAREL, MICHAEL LOWE, HIRANDEEP KUCHOOR, SURYA NALAMATI, AND SHANTHI IYER .....	41
PITCH-DEPENDENT STUDY OF PATTERNED GAASBN NANOWIRES USING BOLTZMANN SIGMOIDAL MODEL .....	42
SEAN JOHNSON, RABIN POKHAREL, MICHAEL LOWE, HIRANDEEP KUCHOOR, SURYA NALAMATI, AND SHANTHI IYER .....	42
GROWTH COBALT OXIDE NANOGRAN ON ALIGNED ELECTROSPUN N-DOPED NANOFIBER FOR ELECTROCHEMICAL DETECTION OF DOPAMINE SECRETED BY LIVING CELLS .....	43
ZIYU YIN, JIANJUN WEI .....	43
BIO-INSPIRED SOFT MULTI-SCALE CAPACITIVE STRESS SENSOR BASED ON DUAL STRUCTURE LIQUID METAL ELASTOMER FOAM.....	44
JIAYI YANG, KI YOON KWON, SHREYAS KANETKAR, MICHAEL D. DICKEY. ....	44
POROUS LIQUID INFUSED SURFACES IN MICROFLUIDICS FOR FLUID DELIVERY: PRESSURE AND HEAT TRANSFER MEASUREMENTS.....	46
REGINALD GOODWIN, BOLAJI SADIKU, JEFFREY ALSTON.....	46
CHARACTERIZING THE PROPERTIES OF GAN- MICROORGANISM BIOINTERFACES.....	47
ALEXEY GULYUK, DENNIS LAJEUNESSE, RAMON COLLAZO, ALBENA IVANISEVIC.....	47
DIFFRACTED DISK REGISTRATION AND LATTICE FITTING FOR CONVERGENT-BEAM ELECTRON DIFFRACTION PATTERNS.....	48
SIHAN WANG, TIM ELDRED, JACOB SMITH, WENPEI GAO .....	48

SPONSORS..... 49



# Carolina Science Symposium

2019

## Organizing Committee

---



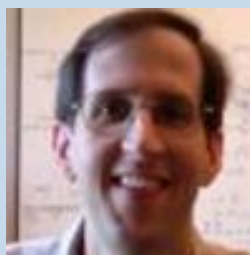
**Fred Stevie**  
Chair  
NC State University  
Raleigh, NC 27695-7531  
[fred\\_stevie@ncsu.edu](mailto:fred_stevie@ncsu.edu)  
919.515.6965 fax



**Dr. John Lannon, Jr**  
Micross Components  
Research Triangle Park,  
NC 27709  
[John.Lannon@micross.com](mailto:John.Lannon@micross.com)  
919. 248.1872



**Joe Becker**  
Vendor Liaison  
Kurt Lesker Company  
[joeb@lesker.com](mailto:joeb@lesker.com)  
919. 889.9099



**Dr. Charles Parker**  
Duke University  
Durham, NC  
[cbparker@duke.edu](mailto:cbparker@duke.edu)



**Roberto Garcia**  
Vice Chair  
NC State University  
Raleigh, NC 27695  
[rgarcia@ncsu.edu](mailto:rgarcia@ncsu.edu)  
919.515.8628



**Dr. Bob Geil**  
UNC at Chapel Hill  
[bob.geil@unc.edu](mailto:bob.geil@unc.edu)  
919.843.6555



**Dr. Philip Barletta**

Poster Session Chair  
NC State University  
NNF  
pbarlet@ncsu.edu



**Dr. Shanthi Iyer**

North Carolina A&T  
Greensboro, NC  
iyer@ncat.edu



**Toby Tung**

NC State University  
toby\_tung@ncsu.edu



**Andy Newell**

Photo Contest Organizer  
andrew.p.newell@gmail.com



**Dr. Maude Cuchiara**

Advertising  
NC State University  
RTNN  
maude\_cuchiara@ncsu.edu



**Phillip Strader**

Vendor Liaison  
NC State University  
RTNN  
phillip\_strader@ncsu.edu



**Dr. Daniel Herr**

Nanoscience Dept  
JSNN  
djherr@uncg.edu



**Chuck Mooney**

Session Chair  
NC State University  
Raleigh, NC 27695-7531  
cbmooney@ncsu.edu



**Anna Lumpkin**

Web Master  
NC State University  
arlumpkin@ncsu.edu

## Awards

Award	Description	Prize
<b>AIF Best Paper Awards</b>	2 awards for the best paper published during the year that acknowledges the use of the Analytical Instrumentation Facility sponsored by <i>AIF</i>	\$200/ea
<b>Student Oral Session Prize</b>	For the best student oral presentations per session (4 sessions total)	\$100/ea
<b>Best Overall Oral Prize</b>	For best Oral presentation across both days, Sponsored by AVS Mid-Atlantic	\$500
<b>2<sup>nd</sup> Place Oral</b>		\$300
<b>3<sup>rd</sup> Place Oral</b>	2 awards	\$100/ea
<b>Student Poster 1<sup>st</sup> Prize</b>	Sponsored by ThermoFisher	\$400
<b>Student Poster 2<sup>nd</sup> Prize</b>	Sponsored by Kurt Lesker	\$200
<b>Student poster 3<sup>rd</sup> Prize</b>	Sponsored by All Scientific (2 awards)	\$100/ea
<b>NNF Best Student Presentation Oral or Poster</b>	Best Student presentation that used the NNF facilities and acknowledged them. Sponsored by <i>NNF</i>	\$200
<b>ASM Hans Stadelmaier Award</b>	Best presentation that shows X-ray Diffraction techniques	\$100
<b>CSS Raffle</b>	2 Drawing randomly from attendees that have filled out the online survey before final awards ceremony.	\$50
<i>Total Awards</i>		<i>\$3,000</i>



## Agenda Nov 12

Time	Presenter	Presentation	
9:00 AM		<b>Introduction</b>	
9:05	Roger Narayan	Biological Microdevices	UNC
9:25		<b>Vendor Presentation by Kurt Lesker (2 videos)</b>	
9:30	Jon Meyers	Patterning hybrid perovskite single crystals by surface-engineered deliquescence and efflorescence	UNC
9:40	Ishita Kamboj	Deterministic Design of Energy Storage Electrodes through Oxide Electrodeposition in CNT Foam Scaffolds	NCSU
9:50		<b>Vendor Presentation by Allied High Tech</b>	
9:55	Younghwan Lee	Unexpectedly Large Remanent Polarization in Ferroelectric Hf <sub>0.5</sub> Zr <sub>0.5</sub> O <sub>2</sub> Capacitor on 002 Textured TiN	NCSU
10:05	Alex Hsain	Control of texture in ferroelectric (Hf, Zr)O <sub>2</sub> thin films using Al <sub>2</sub> O <sub>3</sub> and TiO <sub>2</sub> interlayers	NCSU
10:15	Shisir Devkota	A study of n-doping in MBE grown GaAsSb nanowires using GaTe dopant source and ensemble nanowire near-infrared photodetector	NCA&T
10:25		<b>Session Ends</b>	
1:00pm	Martin King	Biomedical Textiles	NCSU
1:20		<b>Vendor Presentation by ThermoFisher</b>	
1:25	Rabin Pokharel	Dilute nitride Te-doped GaAsSbN nanowire growth and ensemble photodetector application	NCA&T
1:35	Chiung-Wei Huang	Hyperspectral image analysis of graphene derivatives using tip-enhanced Raman spectroscopy	UNC
1:45		<b>Vendor Presentation by Teledyne</b>	
1:50	Salvatore Luiso	An ideal structure for Li-ion battery separators	NCSU
2:00	Mehul Parakh	GaAsSb/GaAs Separate Absorption and Multiplication Nanowire Avalanche Photodiodes for Near-Infrared Photodetection	NCA&T
2:10	Simone Wall	Cellular and Molecular Credentialing of Breast Tumor HER2 Status Using a Cellphone	Duke
2:20		<b>Session Ends</b>	

## Agenda Nov 13

Time	Presenter	Presentation	
9:00 AM		<b>Introduction</b>	
9:05	David Mitzi	New Solar Cell Materials	Duke
9:25		<b>Vendor Presentation by Pfeiffer (2 videos)</b>	
9:30	Eshwar Ravishankar	Achieving Net Zero Energy Greenhouses by Integrating Semitransparent Organic Solar Cells	NCSU
9:40	Kavin Sivaneri Varadharajan Idhaim	Additive Manufacturing of Miniaturized RFID Tag Using Electroceramic Materials for High Temperature Wireless Sensing Applications	WVU
9:50		<b>Vendor Presentation by Physical Electronics</b>	
9:55	Uthpala Herath	Recent developments in PyProcar: A Python library for electronic structure pre/post-processing	WVU
10:05	Mariana Vasquez	Silicate minerals provide non-biological removal of ammonium and phosphate ions from onsite-wastewater-treatment-system effluent	Duke
10:15	Vishal Srikanth	Symmetry-breaking in microscale turbulent porous media flow	NCSU
10:25		<b>Session Ends</b>	
1:00	Heather Splawn	Power Electronics	Kyma
1:25		<b>Vendor Presentation by Protochips</b>	
1:30	Rishabh Guha	Damage Detection in Moisture Contaminated Polymer Composites through Unsupervised Machine Learning	NCSU
1:40	Leo Brody	Ethane to Liquids via a Chemical Looping Approach – Redox Catalyst Demonstration and Process Analysis	NCSU
1:50		<b>Vendor Presentation by Applied Surface Technology</b>	
1:55	Evyn Routh	Growth and characterization of device quality In <sub>x</sub> Ga <sub>1-x</sub> N templates to address droop and red emission in LEDs	NCSU
2:05	Jorge Guerrero	Towards efficient designing of DNA origami nanostructures	NCA&T
2:30		<b>Award Presentations</b>	

## Nov 12 Speakers

---

### Biological Microdevices

Roger Narayan

Two photon polymerization is an additive manufacturing approach that relies on the use of ultrashort laser pulses to selectively polymerize and solidify photosensitive materials. The quadratic character of the two photon absorption probability and the well-defined polymerization threshold of this process allow one to overcome the diffraction limit and obtain structures containing features below one micrometer. Two photon polymerization has recently been used to create several classes of microstructured and nanostructured medical devices out of biocompatible inorganic-organic hybrid materials (e.g., zirconium oxide hybrid materials) and polymers for medical applications. The use of biocompatible photoinitiators (e.g., a combination of riboflavin and triethanolamine) for two photon polymerization will be described. Integration of electrochemical sensors with two photon polymerization-processed devices will be discussed. Evaluation of two photon polymerization-processed materials using *in vitro* biological studies will be considered. In addition, application-specific studies of two photon polymerization-processed medical devices for biosensing, drug delivery, and tissue engineering will be described. Our results indicate that two photon polymerization provides unique benefits for processing medical devices with small-scale features and unique medical functionalities.

## Patterning hybrid perovskite single crystals by surface-engineered deliquescence and

Jonathan K. Meyers, Lorenzo Y. Serafin, Andre Orr, and James F. Cahoon

Lead halide perovskites (LHPs) continue to rise with promise for efficient optoelectronic applications including photovoltaics, radiation detection, and light-emission. A wide variety of deposition techniques and treatments have been developed for LHPs with the goal of improving crystallization and thus efficiency and stability. Of particular interest to us is the exposure of LHP films to methylamine gas. Such treatment has been shown to liquefy the film and dramatically decrease grain boundary defects upon recrystallization. To better understand this reaction, we applied in-situ UV-visible spectrophotometry in controlled conditions of temperature and methylamine gas pressure to obtain a quantitative phase diagram of solid and liquid phases and identified this process as amino-deliqescence and efflorescence. Using in-situ microscopy, we further determined critical thermodynamic and kinetic properties and show dramatic temperature dependence on grain size. Additionally we stress the importance of the liquid-substrate interaction as evidenced by contact angles measured between liquid perovskite and various substrates. Lastly, we demonstrate the utility of these findings in a unique demonstration of solvent-free spin-casting of liquid perovskite into single-crystalline microstructures.

## Deterministic Design of Energy Storage Electrodes through Oxide Electrodeposition in CNT Foam Scaffolds

Ishita Kamboj (1), Michael Spencer (1), Ozkan Yildiz (2), Philip D. Bradford (2), & Veronica Augustyn (1)

(1) Department of Materials Science & Engineering, North Carolina State University

(2) Department of Textile Engineering, Chemistry and Science, North Carolina State University

The use of deterministic design is a growing area of interest to achieve both high energy and power density for energy storage electrodes. Traditionally manufactured energy storage electrodes consist of a multi-component slurry containing an electrochemically active material as well as conductive carbon and polymer binder additives cast onto a flat conductive substrate. Inhomogeneity in the dispersion of the slurry components limits areal power and energy densities due to tortuous and poorly controlled electron and ion transport pathways. In this work, a nanostructured, high capacity transition metal oxide ( $\text{MoO}_3$ ) is electrodeposited onto a conductive carbon nanotube (CNT) foam scaffold to attain high mass loading energy storage electrodes with fast  $\text{Li}^+$  intercalation kinetics. CNT foams provide surface area for the electrodeposition of the  $\text{MoO}_3$  while maintaining sufficient electrical conduction throughout electrodes. Ample porosity between the CNTs provides good ion transport pathways. The  $\text{MoO}_3$  is a model  $\text{Li}^+$  intercalation oxide with a high gravimetric capacity that can be easily electrodeposited from aqueous solutions. This presentation will describe how control over the properties of the CNT foam and  $\text{MoO}_3$  electrodeposition are used to tailor the energy storage performance of the electrode architecture, along with characterization to understand the how the structure of the electrode affects its energy storage behavior. Overall, this research seeks to understand the relationships between electrode architecture and energy storage behavior to achieve simultaneous high power and high energy density.



## Unexpectedly Large Remanent Polarization in Ferroelectric Hf<sub>0.5</sub>Zr<sub>0.5</sub>O<sub>2</sub> Capacitor on 002 Textured TiN

Younghwan Lee, H. Alex Hsain, Gregory Parsons, Jacob L. Jones

The origin of ferroelectricity in HfO<sub>2</sub> has been attributed to the emergence of a polar orthorhombic phase (space group of Pca2<sub>1</sub>) as opposed to non polar monoclinic and tetragonal phases (space group of P2<sub>1</sub>/c and P4<sub>2</sub>/nmc, respectively). It is commonly known that the presence of capping layers, in particular TiN, prevents volumetric expansion of HfO<sub>2</sub> and enables shearing of the HfO<sub>2</sub> unit cell, thereby showing ferroelectricity in Metal-Ferroelectric-Metal (MFM) structure where TiN and HfO<sub>2</sub> serves as metal and ferroelectric layers, respectively. Although numerous papers report the importance of TiN and interface between TiN and HfO<sub>2</sub> layers, not many studies elaborate on the characteristics of their TiN and the interface quality in detail. Here, we introduce a novel Atomic Layer Deposition (ALD) technique referred as Sequential, No Atmosphere Processing (SNAP) to fabricate ferroelectric Hf<sub>0.5</sub>Zr<sub>0.5</sub>O<sub>2</sub> capacitors in MFM structures. SNAP involves the ALD of each layer sequentially (TiN/Hf<sub>0.5</sub>Zr<sub>0.5</sub>O<sub>2</sub>/TiN) while maintaining the sample under vacuum process conditions without ambient exposure during the entire deposition processes. In addition, we report the importance of using 002 textured TiN as bottom and top capping layer which is served as electrode during electrical property measurement. We believe the combined factors of clean interface between TiN and Hf<sub>0.5</sub>Zr<sub>0.5</sub>O<sub>2</sub> layers and unique texture of TiN would be the reason for showing record breaking remanent polarization ( $2P_r \approx 54.2 \mu\text{C}/\text{cm}^2$ ) in ferroelectric Hf<sub>0.5</sub>Zr<sub>0.5</sub>O<sub>2</sub> of 10 nm thickness.

## Control of fiber texture in ferroelectric (Hf, Zr)O<sub>2</sub> thin films using Al<sub>2</sub>O<sub>3</sub> and TiO<sub>2</sub> interlayers

H. Alex Hsain, Younghwan Lee, Greg Parsons, Jacob Jones

Hafnia-zirconia Hf(Zr)O<sub>2</sub> (HZO) ferroelectrics are binary oxides with a simple fluorite structure. While the bulk phase diagram predicts this material system to be dielectric at room temperature, certain driving factors such as dopants, elastic strain, mechanical confinement, or oxygen vacancies have been hypothesized to give rise to the polar, orthorhombic phase (Pca21) responsible for its ferroelectricity. Hafnia ferroelectrics are now being considered for non-volatile memory applications, energy harvesters, actuators, and neuromorphic computing elements. By using a sequential atomic layer deposition (ALD) technique, we have fabricated HZO ferroelectric capacitors of the highest-reported remanent polarization ( $2P_r = 52 \mu\text{C}/\text{cm}^2$ ) with no virtually wake-up effect. However, a critical issue remaining is the high leakage current and poor endurance properties of such high remanent polarization HZO films. In this contribution, we present a method for decreasing leakage current and increasing cycling endurance through the insertion of 1-5 nm dielectric interlayers (ILs) of TiO<sub>2</sub> and Al<sub>2</sub>O<sub>3</sub>. X-Ray Photoelectron Spectroscopy (XPS) and Time of Flight Secondary Ion Mass Spectroscopy (TOF-SIMS) were conducted to determine the degree of distinct and heterogenous layers in the capacitor stack. Not only were the ILs found to influence the electrical and chemical properties of HZO capacitors, but ILs were unexpectedly found to strongly influence the fiber texture of sequentially grown films. Grazing Incidence X-Ray Diffraction (GIXRD) and peak-fitting analysis was conducted to assess the 002/111 peak integral area ratio, finding that the relative 002/111 ratio decreases as a function of increasing IL thickness. The insertion of dielectric ILs is presented as a viable option for controlling and fine-tuning the electrical and structural properties of ferroelectric HZO films.

## A study of n-doping in MBE grown GaAsSb nanowires using GaTe dopant source and ensemble nanowire near-infrared photodetector

Shisir Devkota, Mehul Parakh, Sean Johnson, Priyanka Ramaswamy, Michael Lowe, Aubrey Penn, Lew Reynolds, and Shanthi Iyer

This work reports a comprehensive investigation of the effect of gallium telluride (GaTe) cell temperature variation (TGaTe) on the morphological, optical, and electrical properties of doped-GaAsSb nanowires (NWs) grown by Ga-assisted molecular beam epitaxy (MBE). These studies led to an optimum doping temperature of 550 °C for the growth of tellurium (Te)-doped GaAsSb NWs with the best optoelectronic and structural properties. Te incorporation resulted in a decrease in the aspect ratio of the NWs causing an increase in the Raman LO/TO vibrational mode intensity ratio, large PL emission with an exponential decay tail on the high energy side, promoting tunnel-assisted current conduction in ensemble NWs and significant photocurrent enhancement in the single nanowire. A Schottky barrier photodetector using Te-doped ensemble NWs with broad spectral range and a longer wavelength cutoff at  $\sim 1.2 \mu\text{m}$  was demonstrated. These photodetectors exhibited responsivity in the range of 580 – 620 A/W and detectivity of  $1.2 - 3.8 \times 10^{12}$  Jones. The doped GaAsSb NWs have the potential for further improvement, paving the path for high-performance near-infrared (NIR) photodetection applications.

## Dilute nitride Te-doped GaAsSbN nanowire growth and ensemble photodetector application.

Rabin Pokharel, Priyanka Ramaswamy, Shisir Devkota, Mehul Parakh, Kendall Dawkins, Aubrey Penn, Matthew Cabral, Lewis Reynolds, and Shanthi Iyer

Bandgap engineering of GaAsSbN nanowires (NWs) grown by Ga-assisted molecular beam epitaxy and demonstration of a Te-doped axial GaAsSbN NW-based Schottky barrier photodetector on p-Si (111) in the near-infrared region are reported. Stringent control on NW nucleation conditions, stem growth duration, and NW exposure to the N-plasma were found to be critical for the successful growth of high-quality dilute nitride quaternary GaAsSbN NWs in the axial configuration. Planar defect-free structures were realized with room temperature photoluminescence (PL) characteristics, revealing reduced N-induced point defects and nonradiative recombination centers. N incorporation in the dilute nitride NWs was ascertained from PL and Raman spectral mode shifts and shapes and weak temperature-dependent PL peak energy. The advantage of Te-doping in

dilute nitride NWs using a GaTe captive source is the compensation of point defects, as evidenced by a significant improvement in PL characteristics, Raman mode shifts, and spectral shape, with improved photodetector device performance relative to intrinsic dilute nitride NWs. Te-doped GaAsSbN NW Schottky-based photodetectors have been demonstrated on both single and ensemble configurations with a resultant responsivity of 5 A/W at 860 nm and 3800 A/W at 1100, respectively. Detectivity of  $3.2 \times 10^{10}$  Jones was achieved on the Te-doped ensemble NW device. The findings presented in this work showcase prospects for rich bandgap engineering using doped GaAsSbN NWs for near-infrared region device applications.

## Fiber Cross-sectional Shape Influences the Cellular Response of Surface Treated Biodegradable Biphasic Tissue Engineering Scaffolds for Tendon-Bone Junction Repair.

Martin W. King and Harshini Ramakrishna

Wilson College of Textiles, North Carolina State University, Raleigh, NC 27606

A musculoskeletal interface, such as a tendon-bone junction, is a complex tissue site since it transfers stress from soft flexible tendon tissue to hard mineralized bone, and is therefore prone to injury. And because it connects two very dissimilar types of tissues, the reattachment and permanent repair of torn or severed rotator cuff tendons is still a major clinical challenge. The ultimate goal of this study was to develop a biodegradable biphasic scaffold for tendon-bone junction regeneration using textile technologies and surface treatments. Braiding and knitting technologies were used to design and fabricate bilayer tubular scaffolds from biodegradable poly(lactic acid) yarns with three different fiber cross-sections, namely round, grooved (4DG) and trilobal. The scaffolds were evaluated in terms of their physical and mechanical properties, and their surfaces were activated using radio frequency plasma followed by immobilization of collagen with genipin as a spacer molecule. FTIR, XPS, ToF-SIMS and SEM were used to characterize the activated surfaces. In order to form a structural gradient, hydroxyapatite was coated on one end of the scaffolds to mimic the bone region. The biological performance was evaluated by culturing with mesenchymal stem cells under static and dynamic uniaxial cyclic stretch conditions and measuring the cell viability, proliferation, attachment and gene expression of tenogenic, osteogenic and chondrogenic markers using laser scanning fluorescent confocal microscopy, RT-PCR and the alamarBlue™ assay. In addition, the cell attachment on fibers with different cross-sectional shapes was visualized using optical microscopy, SEM and histological sectioning. The incorporation of collagen and a hydroxyapatite coating promoted bioactivation, improved biocompatibility and differentiation of the mesenchymal stem cells into tendon and bone cells. Furthermore, the trilobal fibers provided an increase in surface area and improved guidance for cell attachment, differentiation and superior stem cell gene expression. In comparison, the round fibers promoted cell proliferation. So this study was the first to report the influence of fiber cross-sectional shape on the biological response of stem cells.



## Hyperspectral image analysis of graphene derivatives using tip-enhanced Raman spectroscopy

Chiung-Wei Huang, Xiao You, Kizhanipuram Vinodgopal, and Joanna M. Atkin

Interest in graphene has grown considerably in the last decade due to its unique optical and electrical properties. However, some potential applications of graphene, such as transistors, require a bandgap, which is challenging to generate in graphene. One strategy is to tune local electronic properties by chemical modification through oxidation and surface functionalization. Using transition metal complexes, a desirable energy gap can be opened up in graphene.

However, understanding and thereby controlling the mechanism of functionalization is hampered by the high degree of structural and chemical disorder in graphene and graphene derivatives. Pure graphene contains inhomogeneous morphological defects such as grain boundaries, edges, and wrinkles. Engineering the electronic properties by surface modification can often lead to a larger degree of inhomogeneity in chemical composition, molecular structures, and the degree of sp<sup>2</sup> conjugation.

Since the number of molecules needed for chemical modification is low, macroscopic methods such as energy-dispersive X-ray spectroscopy or X-ray photoelectron spectroscopy lack the spatial and chemical sensitivity necessary to detect modifications in graphene.

In this work, we employ functional scanning probe microscopy (SPM) techniques that offer spatially resolved, chemically specific and quantitative information on chemically modified graphene derivatives.

Tip-enhanced Raman spectroscopy (TERS) is a powerful surface analysis technique that offers nanometer-resolved images with site-specific chemical fingerprints. We demonstrate nanoscale TERS mapping of structural and functional groups on graphene derivatives. We employ machine learning (ML) tools to extract information on chemical components and their spatial distribution from the hyperspectral TERS maps.

We validate the components resulted from ML-aided analysis by comparing the principal components with density functional theory (DFT) based calculation. The prediction of vibrational modes from DFT offers insights into understanding the site-specific derivative molecules and the bonding between molecules and graphene.

These methods can be applied to correlated SPM data to obtain complex compositional information that is challenging to gain from any conventional method. By combining nanometer-resolved TERS, computation-aided ML and analysis, we have offered a comprehensive view of chemical and spatial information and demonstrated a generally applicable approach for improving the accuracy of surface characterization. We expect this work to provide a more profound understanding of the molecular binding structures with guidance for optimizing graphene semiconductors and devices.

## An ideal structure for Li-ion battery separators

Salvatore Luiso, Austin Williams, Orlin Velez, Behnam Pourdeyhi, Peter Fedkiw

Among all types of Li-ion battery (LIB) separators, fibrous mats have the advantage of low cost, low mass, and high porosity. Fibrous Poly(Vinylidene difluoride) (PVDF) shows promising results because of its stability and affinity for electrolytes commonly employed in Li-ion cells. Despite numerous studies published on fibrous LIB separators, none reports structure-property relationships for the identification of an ideal structure. We investigated the properties of a melt-blowable PVDF and produced meltblown PVDF mats in scale-up equipment with the objective of elucidating its performance as a LIB separator. We also present a new class of LIB separators, PVDF-based highly-branched, colloidal polymer particulates called soft dendritic colloids that are produced by shear-driven polymer precipitation within a highly turbulent nonsolvent flow, followed by filtration. We show that the morphology of the resulting PVDF particulates can be modulated from fibrous soft dendritic colloids (SDC) to thin and highly porous sheet-like particles.

Through a scale-up system, we obtained high-quality meltblown PVDF with high homogeneity, low number of defects, an average fiber diameter of 1.4  $\mu\text{m}$ , and pore size as low as 0.9  $\mu\text{m}$ . Small fiber diameter provides high-surface area and high-electrolyte uptake. We show interactions of the meltblown PVDF with the electrolyte lead to a morphology change in the fibers. The highest ionic conductivity was  $\sim 9.6 \text{ mS/cm}$ , and the first-cycle capacity was 140 mAh/g (Li/LiCoO<sub>2</sub>). After melt-pressing, the thickness and pore size decrease, but the mats electrolyte absorbency and conductivity decrease commensurately. PVDF SDC separators show high porosity (up to 80%) and high particle surface area, which results in high conductivity (1.2 mS/cm), high-electrolyte uptake (325%), and high-cell capacity (112 mAh/g in Li/LiCoO<sub>2</sub> cell) with <10% loss after 50 cycles. Both processes yield separators with low thermal shrinkage (<5% at 90 °C) and high tensile strength (<0.5% offset at 1000 psi), with the highest-performing separator possessing low average fiber diameter with a wide diameter distribution.

Both meltblowing and shear-driven precipitation are facile and versatile processes for high-volume fabrication of LIB separators with one single polymer without necessarily requiring post-processing and with characteristics similar to commercially available battery separators. Fibrous LIB separators should be fabricated with a low fiber diameter (<1  $\mu\text{m}$ ) but also with a wide diameter distribution. When the strength and openness of the microfiber support is coupled with the highly permeable nanofibers for a low average pore size, an ideal fibrous Li-ion battery separator is obtained.

## GaAsSb/GaAs Separate Absorption and Multiplication Nanowire Avalanche Photodiodes for Near-Infrared Photodetection.

Mehul Parakh, Rabin Pokharel, Priyanka Ramaswamy, Hirandeep Kuchoor, Jia Li and Shanthi Iyer

Avalanche photodiodes (APDs) are key components in optical communication systems, quantum key distribution systems and active imaging system requiring both ultrafast response time to measure photon time of flight and a high gain to detect low photon flux. However high internal gain in APDs increase the excess noise, thereby impacting the overall signal to noise ratio of the device. This preliminary work demonstrates the first self-catalyzed growth of GaAsSb/GaAs separate absorption and multiplication nanowire APDs grown on lithography free Si substrate for future CMOS compatibility and excess noise reduction. A varying gain of 80-100 was demonstrated using C-AFM analysis for single nanowire APDs at 633nm at -8 V. This work presents a clear path towards fabricating high performance as-grown ensemble nanowire APD device grown on Si substrate for near-infrared photodetection.

## Cellular and Molecular Credentialing of Breast Tumor HER2 Status Using a Cellphone

Simone A. Wall, Jacob T. Heggstad, Daniel Y. Joh, Shengwei Zhang, E. Shelley Hwang, Kyle C. Strickland, Qingshan Wei, Ashutosh Chilkoti

Breast cancer (BC) is the leading cause of cancer mortality among women. The burden of BC is especially high in limited-resources settings (LRS), where roughly half of the cases and a majority of the deaths occur. Effective management of BC requires detailed histopathological and molecular assessment of the tumor to inform treatment and prognosis. For example, elevated expression of human epidermal growth receptor 2 (HER2) on BC tumors makes them more susceptible to trastuzumab, a drug targeting HER2. Unfortunately, detailed molecular and cellular assessment of BC tumors is often unavailable in LRS, leading to poor patient outcomes. To address this unmet need, we developed a portable, point-of-care system—the EpiView-D4—for cellular and molecular credentialing of tumors for use in LRS. The EpiView-D4 consists of two innovative components: (1) an immunodiagnostic chip (the “D4”) which quantifies expression of protein biomarkers, such as HER2. The D4 assay is a self-contained immunoassay built upon a “nonfouling” polymer brush-coating, enabling picomolar sensitivity of protein analytes from complex mixtures. (2) A custom cellphone-based optical microscope (the EpiView) that allows brightfield imaging of BC cytology preparations and performs readout of D4 assay fluorescence. We used the EpiView-D4 to image cytology preparations and assess HER2 expression levels directly from tumor fine needle aspirations (FNA), the sampling method of choice in LRS. Device performance was evaluated in cancer cell lines, animal models, and human tissue specimens.

First, we demonstrated the sensitivity of the D4 platform by constructing a calibration curve (fabricated with commercial anti-HER2 antibodies) that was run in a lysis buffer (RIPA) spiked with varying amounts of recombinant HER2. We observed a sensitivity of 12 pM and dynamic range spanning over 3 logs. The performance was further validated using established BC human cell lines. We next tested the ability of the combined platform to assess both cytopathology and HER2 expression levels from orthotopically implanted BT474, MDA-MB-453, or BT20 cells in nude mice. We found that our device was able to reliably distinguish differences in HER2 expression across BT474, MDA-MB-453, and BT20 xenografts. In addition, we observed the relative D4 fluorescence signal between xenograft groups matched the relative HER2 expression patterns assessed by western blotting and that there was a strong, positive correlation between D4 and ELISA measurements. Finally, we tested FNA samples from 19 human breast tissue specimens archived at Duke University Medical Center. We found that EpiView brightfield images of cytology smears were adequate for pathological assessment of lesional cellularity and tumor content. Further, we were able to accurately categorize HER2 negative and HER2 positive tumors. Taken together, the EpiView-D4 offers a promising alternative to invasive—and often unavailable—pathology services and may enable the democratization of effective breast cancer management in LRS.

## Ethane to Liquids via a Chemical Looping Approach – Redox Catalyst Demonstration and Process Analysis

Leo Brody\*, Luke Neal\*, Vasudev Haribal, and Fanxing Li

(\*=co-first authors)

The inability to economically transport ethane from distributed shale gas production results in the “rejection”, i.e. flaring or reinjection, of this important petrochemical feedstock. Therefore, a technology capable of efficiently converting geographically isolated ethane into transportable liquid fuels would effectively exploit this abundant yet wasted resource. We proposed a modular ethane-to-liquids (M-ETL) system that employs a chemical looping-oxidative dehydrogenation (CL-ODH) scheme to convert ethane into olefins via cyclic redox reactions. The olefins would subsequently undergo oligomerization to form mid-distillate liquid fuels. In this study, a sodium molybdate promoted  $\text{CaTi}_{0.1}\text{Mn}_{0.9}\text{O}_3$  core-shell redox catalyst ( $\text{CaTi}_{0.1}\text{Mn}_{0.9}\text{O}_3@\text{Na}_2\text{MoO}_4$ ) is presented as a potentially viable, redox-active catalyst for the CL-ODH of ethane to ethylene. Performance data were collected from 1,600+ hours (>4,000 CL-ODH cycles) of catalyst performance at operating temperatures ranging between 700 and 750°C and varying gas hourly space velocities. 52 – 58% single-pass olefin yields at 725 and 730°C were obtained with relatively low (2.5 – 8%)  $\text{CO}_x$  selectivity. The experimental data were used as inputs to an ASPEN Plus® based M-ETL system model to evaluate its performance. Sensitivity analyses were performed on the CL-ODH and oligomerization sections of the M-ETL system, and the results were used to inform economic analysis of the process.



## Nov 13 Speakers

---

### Versatile Perovskite Semiconductors

David B. Mitzi<sup>1,2</sup>

1 Department of Mechanical Engineering and Materials Science, Duke University, Durham, NC USA

2 Department of Chemistry, Duke University, Durham, NC USA

Halide-based hybrid perovskites offer an unprecedented degree of tunability through mixing and matching of diverse functionalities for inorganic and organic components and have seen a rapid rise in interest for use in solar cells, light-emitting devices, detectors and other applications. This talk will introduce this versatile semiconductor family and briefly discuss several ways in which the organic structural component can be used to tailor the functional aspects of the materials. As one example, selection of an appropriate chiral organic cation may lead to a transfer of chirality from the organic to the inorganic structural component, leading to a breaking of symmetry within the inorganic layer and a large Rashba-Dresselhaus splitting of the conduction band. Such versatility yields new opportunities for fundamental science and prospective device applications.

## Achieving Net Zero Energy Greenhouses by Integrating Semitransparent Organic Solar Cells

Eshwar Ravishankar, Ronald E. Booth, Carole Saravitz, Heike Sederoff, Harald W. Ade, and Brendan T. O'Connor

Greenhouses vastly increase agricultural land-use efficiency. However, they also consume significantly more energy than conventional farming due in part to conditioning the greenhouse space. One way to mitigate the increase in energy consumption is to integrate solar modules onto the greenhouse structure. Semitransparent organic solar cells (OSCs) are particularly attractive given that their spectral absorption can be tuned to minimize the attenuation of sunlight over the plants photosynthetically active spectrum. Here, the benefits of integrating OSCs on the net energy demand of greenhouses within the U.S. are determined through a detailed energy balance model. We find that these systems can have an annual surplus of energy in warm and moderate climates. Furthermore, we show that sunlight reduction entering the greenhouse can be minimized with appropriate design. These results demonstrate that OSCs are an excellent candidate for implementing in greenhouses and provide an opportunity to diversify sustainable energy generation technology.

## Additive Manufacturing of Miniaturized RFID Tag Using Electroceramic Materials for High Temperature Wireless Sensing Applications

Kavin Sivaneri Varadharajan Idhaian, Domenic Cipollone, Edward M. Sabolsky, Konstantinos Sierros, Daryl Reynolds

The primary objective of this work focused on analyzing the parameters that affect the resolution of nozzle based direct ink writing of miniaturized RFID tags for wireless temperature sensing at high temperatures. The inks were made by dispersing the electroceramic particles of size  $< 7\ \mu\text{m}$  in various organic vehicles. Different volume loadings of the electroceramic particles were evaluated to maximize the solid loadings to achieve high density after post-processing. The parameters that affect the process such as viscosity, wettability, print rate, and particle size were evaluated. A planar inductor coil consisting of 15 turns with  $170 - 180\ \mu\text{m}$  line width and  $\sim 200\ \mu\text{m}$  spacing was deposited on an alumina substrate to demonstrate the capability of the process. The patterned substrates were sintered at temperatures  $> 1000^\circ\text{C}$  for further characterization. A suite of characterization was performed by particle size analyzer, rheometer, contact angle measurement, SEM, XRD, and impedance spectroscopy.

## Recent developments in PyProcar: A Python library for electronic structure pre/post-processing

Uthpala Herath, Pedram Tavadze, He Xu, Eric Bousquet, Sobhit Singh, Reese Boucher, Logan Lang, Freddy Farah, Francisco Muñoz, Aldo H. Romero

We present our recent updates to PyProcar, a robust, open-source Python package providing graphical representations for electronic structure calculations. PyProcar is capable of performing a multitude of tasks including plotting plain and spin/atom/orbital projected band structures and Fermi surfaces (in 2D and 3D), unfolding bands of a super cell into predefined unit cell, comparing band structures from multiple DFT calculations, plotting PDOS and generating a k-path for a given crystal structure. Additionally, PyProcar plots Fermi surfaces which map colors depending on other properties (e.g. electron velocity, electron-phonon mean path, effective mass) when provided a file with a desired specific property evaluated for each k-point in a k-mesh and for each band. PyProcar can be conveniently used in a stand-alone command line mode or a library mode, accessible through the Python packaging index and conda. It currently supports VASP, Elk, Quantum Espresso, Abinit and Lobster.

## Silicate minerals provide non-biological removal of ammonium and phosphate ions from onsite-wastewater-treatment-system effluent

Vasquez, Mariana; Hawkins, Brian T.; Trotochaud, Lena

Treated sewage exiting from non-sewered sanitation systems (NSSS) contains high levels of nitrogen and phosphorus (primarily as ammonium and phosphate) which can contribute to eutrophication. Eutrophication not only represents a threat for the ecosystem, but also a significant economic cost and can be directly hazardous to human health. Consequently, new standards for water discharge and reuse for NSSS have been adopted, such as the ISO 30500 which require 70% and 80% reduction in total N and P, respectively. Nutrient removal in small scale systems can be challenging and costly because the most effective known methods are designed for large scale systems and rely on biological processes. An exciting option for a non-biological nutrient removal in NSSS is the use of natural silicate-based mineral sorbents. We investigated clinoptilolite and Polonite which sorb ammonium and phosphate, respectively, for nutrient removal from blackwater. Lab-scale batch experiments were carried out using raw blackwater and blackwater pre-treated with granular activated carbon and ultrafiltration. Results indicate clinoptilolite and Polonite are effective in the removal of the targeted nutrients at small loading for pre-treated blackwater. Clinoptilolite and Polonite regeneration were attempted using 1 M HCl and 1 M KOH, respectively. Clinoptilolite capacity could be recovered at >70%, while only ~20% of Polonite capacity could be recovered, indicating that ion exchange is not the dominant mechanism of phosphate removal by Polonite. Both materials were incorporated in full-scale lab testing with a prototype wastewater treatment system achieving >80% and >60% removal of ammonium and phosphate, respectively. Based on these encouraging results, we will discuss the implications for both sorbent materials in pilot and field testing of NSSS.



## Symmetry-breaking in microscale turbulent porous media flow

Vishal Srikanth, Ching-Wei Huang, Timothy S. Su, Andrey V. Kuznetsov

Microscale turbulence in porous media is a new physical phenomenon that exhibits unique properties unlike those in classical turbulence flows. At low values of porosity, the surface forces on the solid obstacles compete with the inertial force of the fluid flow to result in the formation of flow instabilities. In this paper, we report the origin and mechanism of a symmetry-breaking phenomenon in periodic porous media that causes a deviation in the direction of the mean flow from that of the applied pressure gradient. Large Eddy Simulation (LES) is used to simulate turbulent flow in a homogeneous porous medium consisting of a periodic, square lattice arrangement of cylindrical solid obstacles. Direct Numerical Simulation (DNS) is used to simulate the transient stages during symmetry breakdown and also to validate the LES method. Quantitative and qualitative observations are made from the following approaches – (1) macroscale momentum budget, (2) 2D & 3D flow visualization. The phenomenon draws its roots from the amplification of a flow instability that emerges from the vortex shedding process. The symmetry-breaking phenomenon is a pitchfork bifurcation that can exhibit multiple modes depending on the local vortex shedding process. The phenomenon is observed to be sensitive to the porosity, solid obstacle shape, and the Reynolds number. It is a source of macroscale turbulence anisotropy and flow field disorientation in porous media for symmetric solid obstacle geometries. Thus, symmetry-breaking in porous media involves new flow physics that should be taken into consideration while modeling flow inhomogeneity in the macroscale.

## Growth and characterization of device quality $\text{In}_x\text{Ga}_{1-x}\text{N}$ templates to address droop and red emission in LEDs

Evyn Lee Routh, Mostafa Abdelhamid, N.A. El-Masry, S.M. Bedair

A semiconductor material system with a bandgap that spans the whole visible spectrum is desirable for optoelectronic and solar cell applications. III-Nitride based devices are an excellent candidate for this task, as LED devices based on the  $\text{In}_x\text{Ga}_{1-x}\text{N}$  alloy have shown to be successful in the blue-emitting region. A major challenge that faces the realization of green and red emitting III-Nitride LEDs is the strain introduced due to the lattice mismatch between the  $\text{In}_x\text{Ga}_{1-x}\text{N}/\text{GaN}$  multiple quantum wells (MQWs) and the underlying substrate used for epitaxial growth, as well as the material degradation of the  $\text{In}_x\text{Ga}_{1-x}\text{N}$  alloy when  $x$  reaches values necessary for longer wavelength emission. We present  $\text{In}_x\text{Ga}_{1-x}\text{N}$  templates utilizing the semi-bulk growth approach that allows for transition from strain to strain-relaxation of the heterostructure, resulting in a lattice parameter that is closer to that of the QWs. The semi-bulk growth consists of a periodic structure of  $\text{InGaN}$  followed by a  $\text{GaN}$  interlayer that is below the critical layer thickness. However, the mechanism in which  $\text{InGaN}$  relaxes is the formation of V-pits, an open 6-sided hexagonal faced defect. These V-pits often nucleate at threading dislocations that propagate through the heterostructure as the growth progresses. The  $\text{GaN}$  interlayer acts as a back-filling agent, mitigating the impacts of the V-pits on the QW growth. An  $\text{In}_x\text{Ga}_{1-x}\text{N}$  semibulk template with an indium content of  $x \sim 7\text{-}10\%$  as estimated from photoluminescence (PL) emission in the range of 409-420 nm is presented, with an RMS surface roughness measured via atomic force microscopy (AFM) of approximately 2.7 nm across a  $(5 \mu\text{m})^2$  area. The threading dislocations are characterized via high-resolution x-ray diffraction (HRXRD) omega-scans, and are reported to be in the regime of  $10^8 \text{ cm}^{-2}$  for our template. The etch-pit density (EPD) quantified via AFM by utilizing a silane etch protocol, and is found to be in the  $10^8 \text{ cm}^{-2}$ . Work towards and preliminary results of higher indium content  $\text{In}_x\text{Ga}_{1-x}\text{N}$  templates (target PL emission  $\sim 440 \text{ nm}$ ) is also presented. These templates when used as substrates for MQWs will address two major problems in LEDs: droop and poor-quality red emission.

## Emerging Wide Bandgap Semiconductor Materials

Heather Splawn, KYMA

This talk will provide an overview of emerging wide bandgap semiconductors and their applications. While SiC has been adopted in several high volume applications, GaN, AlN, and Ga<sub>2</sub>O<sub>3</sub> are now emerging as next generation materials for certain applications. The state of the art for these materials will be introduced as well as Kyma's role in the development of these exciting markets.

## Damage Detection in Moisture Contaminated Polymer Composites through Unsupervised Machine Learning

Rishabh D Guha, Katherine Berkowitz, Ogheneovo Idolor, Dr. Landon Grace

Non-destructive evaluation techniques in composites is becoming extremely crucial in determining the location and extent of damage for in-service polymer composites. In this work, an attempt has been made to use the relative permittivity of moisture as an imaging agent to detect damage in a polymer composite. Localized damage is induced in the laminate specimens via low velocity impact damage of 9 Joules. A split post dielectric resonator coupled with a vector network analyzer has been used to determine the spatial variation in relative permittivity across the composite laminate. Generally, results show significant increase in relative permittivity towards the damage location compared to surrounding undamaged areas. This increase is indicative of internal damage as a result of micro-crack formation around the point of impact and the new free volume in the damaged area is primarily occupied by “free” water molecules which are characterized by a higher relative permittivity; driving a local increase in the permittivity due to the higher ratio of free to bound water. The tendency of polymer composites to absorb moisture in almost all environments coupled with the high sensitivity of our technique makes this relatively simple non-destructive examination novel, especially for the early detection of damage.

For this work, we have tried to use unsupervised machine learning to perform a clustering analysis on the permittivity data collected to detect the damage spot and delineate a damage boundary.

## Towards efficient designing of DNA origami nanostructures

Jorge Guerrero, Reza Zadegan

DNA origami is a promising tool for the bottom-up design of self-assembly nanostructures. Our imagination and skills to handle this technique delimit the vast possible uses. Given the increased interest in DNA origami, several software applications have been developed to assist during the design process. Most of them require manual guidance and verification of each detail from the user's point of view, reducing the chance of bigger and complex designs. To address these issues, we created MENDEL, a software library that automates the process of designing DNA nanostructures. MENDEL provides a sequence of commands bringing the capability of a parametric description of the geometry, size, and shape; reducing time, error, and computational cost during the designing process. MENDEL can generate the previsualization of the design when running under Blender. For convenience, MENDEL generates caDNAno and CanDo compatible files. We aim to maintain MENDEL as an opensource project and allow community collaboration and be accessible to a wide range of scientists.

## Posters

#	Presenter	Title	
1	Priyanka Ramaswamy	Electrical and Surface Analysis of MBE Grown Intrinsic and Te-Doped GaAsSb Nanowires	<i>NCA&amp;T</i>
2	Tim Eldred	Enhancing the Spatial Resolution of Nano Beam Electron Diffraction Phase Mapping	<i>NCSU</i>
3	Sajedeh Pourianejad	Work function modulation in 2D MoS2	<i>UNCG</i>
4			
5	Kirby Schmidt	Advanced Strain analysis of Graphene on in Van der Waals heterostructures	<i>UNC, JSNN</i>
6	Saeed Saeed	Deformation of Prussian Blue during Electrochemical Cation Insertion from Aqueous Electrolytes	<i>NCSU</i>
7	Kendall Dawkins	A Simulation Study of Carrier Induced Change in Refractive Index for Optimal Light Absorption in GaAsSb Nanowires	<i>NCA&amp;T</i>
8	Gayani Chathurika Pathiraja	Greener synthesis of high aspect ratio copper oxide nanowires for potential applications	<i>UNCG, JSNN</i>
9	Sean Johnson	Pitch-Dependent Study of Patterned GaAsSbN Nanowires using Boltzmann Sigmoidal Model	<i>NCA&amp;T</i>
10	Ziyu Yin	Growth cobalt oxide nanograin on aligned electrospun N-doped nanofiber for electrochemical detection of dopamine secreted by living cells	<i>UNC</i>
11	Shreyas Kanetkar	Bio-inspired Soft Multi-scale Capacitive Stress Sensor based on dual structure Liquid Metal Elastomer Foam	<i>NCSU</i>
12	Reginald Godwin	Porous liquid infused surfaces in microfluidics for fluid delivery: Pressure and heat transfer measurements	<i>NCA&amp;T</i>
13	Alexey Gulyuk	Characterizing the properties of GaN-microorganism biointerfaces	<i>NCSU</i>
14	Sihan Wang	Diffraction Disk Registration and Lattice Fitting for Convergent-Beam Electron Diffraction Patterns	<i>NCSU</i>

Electrical and Surface Analysis of MBE Grown Intrinsic and Te-Doped GaAsSb Nanowires

Priyanka Ramaswamy, Shisir Devkota, Rabin Pokharel, Surya Nalamati, Keith Jones, Jia Li, and Shanthi Iyer.

In this paper, photoresponse of intrinsic GaAsSb, Te-doped GaAsSb, GaAsSbN, and Te-doped GaAsSb nanowires (NWs) on p- Si (111) and graphene/SiO<sub>2</sub>/p- Si (111) substrates, which are grown by molecular beam epitaxy (MBE), are investigated using conductive atomic force microscopy (C-AFM). The topographical and electrical characteristics of the vertical single nanowire are demonstrated using C-AFM. Responsivity, detectivity, and external quantum efficiency of intrinsic and Te-doped nanowires are analyzed using current-voltage characteristics. Responsivity of intrinsic GaAsSb, GaAsSbN on p- Si (111) and GaAsSb on graphene/SiO<sub>2</sub>/p- Si (111) is found to be 0.08 A/W, 0.1 A/W and 0.53 A/W, respectively. Responsivity of Te-doped GaAsSb, GaAsSbN on p- Si (111) and GaAsSb on graphene/SiO<sub>2</sub>/p- Si (111) is found to be 0.12 A/W, 5 A/W and 2 A/W, respectively. The increase in responsivity confirms the presence of Tellurium dopants in NWs. Also, intrinsic and Te-doped GaAsSb NWs are investigated and characterized by X-ray photoelectron spectroscopy (XPS) and ultraviolet photoelectron spectroscopy (UPS). It was found that by using a Gaussian-Lorentzian convolution with a Smart-type background, a positive shift in binding energy in XPS spectra is observed, thereby confirming the incorporation of Te dopants in GaAsSb NWs. From Te-doped GaAsSb UPS spectra, a shift in Fermi level towards the conduction band further evidenced the high doping of Te in GaAsSb NWs and also, the carrier concentration was found to be in the order  $10^{19} \text{ cm}^{-3}$ . As Hall effect, field-effect, and capacitance-voltage measurements require good ohmic contacts, which are quite challenging in the case of NWs, a combination of contactless methods such as XPS, UPS and C-AFM are other convenient techniques to determine different intrinsic physical properties that are critical to bandgap engineering design of opto-electronic devices.

#### Acknowledgement

This material is based upon research supported by the Air Force Office of Scientific Research (AFOSR) under grant number W911NF1910002.



## Enhancing the Spatial Resolution of Nano Beam Electron Diffraction Phase Mapping

Tim B. Eldred, Jacob G. Smith, Wenpei Gao

As new techniques of material characterization are introduced, methods to optimize spatial resolution while maintaining usability become critical. Nanobeam Electron Diffraction (NBED) has been used as a method of characterizing local phase information in materials by evaluating the breaks in symmetry. Barium Titanate (BTO) has been used as one of the target materials for this method, due to the order-disorder phase transition mechanism, that results in nanoscale regions of lower symmetry inside of nano- to microscale regions of higher symmetry. By using 4DSTEM, diffraction patterns can be acquired over a region of the sample, and then analyzed for symmetry to differentiate between the lower (rhombohedral) and higher (tetragonal) symmetry regions. Methods using analysis of mirror symmetry in the resulting patterns, as well as methods using the relative intensity in the second order reflections have been used to confirm the method, but both report limits to the spatial resolution of their scan that hinder full analysis. [1,2] Since the regions of interest in the NBED patterns are the dynamic diffraction information in the discs, imaging conditions are performed with a low convergence angle to avoid overlap. This results in a probe with a FWHM of 7+ angstrom, leading to a 3x3 unit cell area being partially sampled at each position, and limiting the spatial resolution of the data. We have demonstrated a method of masking out the overlapping regions at higher convergence angles, resulting in equivalent patterns to the lower convergence angle data while maintaining the spatial resolution of the higher convergence angle data. This results in a projected 3 angstrom probe size, and a spatial resolution of ~1 unit cell.

1) Shao, Y.-T., et. al. <https://doi.org/10.1107/S2052520617008496>.

2) Tsuda, Kenji, et. al. <https://doi.org/10.1063/1.4819221>.

## Work function modulation in 2D MoS<sub>2</sub>

S. Pourianejad, J. Averitt, T. Ignatova

Two-dimensional (2D) molybdenum disulfide (MoS<sub>2</sub>) has drawn a lot of attention due to its tunable electrical and optical properties, resulting in various applications such as field effect transistors, and photodetectors. Importantly, the intrinsic optical properties could be enhanced by modifying the electronic structure of the 2D MoS<sub>2</sub> with proper doping. Doping results in the charge transfer and the Fermi level shift, leading to a work function (WF) modulation. A comprehensive analysis of the electronic band structure and control over the WF of 2D components are crucial, resulting in better performance of potential devices. Here, we focus on the study of the band alignment of 2D MoS<sub>2</sub> before and after doping. To ascertain the MoS<sub>2</sub> layer number and defects, confocal Raman spectroscopy and Photoluminescence (PL) measurements were conducted. Sample thickness was determined by atomic force microscopy measurement. Scanning electron microscopy was used to investigate the surface morphologies of MoS<sub>2</sub>. To investigate work function and charge-related phenomena on surfaces, Kelvin probe force microscopy (KPFM) was carried out. In conclusion, we found that p-doping can enhance PL and increase the WF of 2D MoS<sub>2</sub>.

## Advanced Strain analysis of Graphene on in Van der Waals heterostructures

Kirby Schmidt, Sajedah Pourianejad, Anthony Trofe, Tetyana Ignatova

Graphene's electronic band structure is extremely sensitive to small perturbations in its crystal lattice. Because of this it is vital to correctly characterize strain, doping and defects in graphene through nondestructive measurements. Graphene on Transition Metal Dichalcogenides (TMDCs) show increased strain which is not caused by defects introduced through the transfer method. We prove this using Raman analysis of graphene samples on silicon oxide and MoS<sub>2</sub>. Graphene shows G peak splitting and shift indicative strain increasing on top of MoS<sub>2</sub> when compared to nearby graphene on SiO<sub>2</sub>. We separate strain components into their hydrostatic and shear components. We also analyze substrate induced strain and doping of MoS<sub>2</sub> and its correlation with graphene strain.

This work was performed at the Joint School of Nanoscience and Nanoengineering (JSNN), a member of the Southeastern Nanotechnology Infrastructure Corridor (SENIC) and National Nanotechnology Coordinated Infrastructure (NNCI), which is supported by the National Science Foundation (Grant ECCS-1542174).

## Deformation of Prussian Blue during Electrochemical Cation Insertion from Aqueous Electrolytes

Saeed Saeed, Shelby Boyd, Wan-Yu Tsai, Ruocun Wang, Nina Balke, and Veronica Augustyn

Prussian blue ( $\text{Fe}_4[\text{Fe}(\text{CN}_6)]_3$ ) and its analogues are of interest as electrode materials for electrochemical energy storage. The open cubic framework of Prussian blue allows for long cycle life and reversible intercalation kinetics during cation insertion/extraction with capacities of up to 125 mAh/g in aqueous electrolytes. However, this performance is highly dependent on the electrolyte cation, and prior results indicate that a smaller hydrated cation radius leads to the best cyclability. The hypothesis guiding this study is that the cycling stability of ions with lower hydration energies is tied to lower structural deformation of Prussian blue during electrochemical intercalation. In this study, we investigate the electrochemomechanics of Prussian due to the intercalation of three different aqueous cations,  $\text{K}^+$ ,  $\text{Na}^+$ , and  $\text{Li}^+$ . Operando atomic force microscopy (AFM) is used to measure the mechanical deformation of the electrode during electrochemical cycling as a function of electrolyte and cyclic voltammetry sweep rate. This technique confirms that the electrochemical stability as well as the local deformation of the Prussian blue is dependent on the hydrated cation radius, with smaller cations giving rise to larger deformation. The superior cycling stability seen during  $\text{K}^+$  insertion is commensurate with the high mechanical stability measured via operando AFM. This presentation will provide an understanding of the coupling between electrolyte cation size and electrochemomechanical response of a framework-type energy storage material.

## A Simulation Study of Carrier Induced Change in Refractive Index for Optimal Light Absorption in GaAsSb Nanowires

Kendall Dawkins

Lumerical Finite-Difference Time-Domain modeling has been used to simulate the absorption characteristics of P-I-N axial and core-shell gallium arsenide antimonide (GaAsSb) nanowires. A Kramer-Kronig's analysis was used to determine the change in refractive index and extinction coefficient for a GaAsSb thin film of different doping concentrations, which was then used to simulate the absorption characteristics in the nanowire configuration. It was found that increasing n-type doping decreases the absorption percentage when the n- segment forms the outermost part (shell) of the nanowire configuration. The optimal absorbance spectra for GaAsSb nanowires for arrays was determined by varying nanowire diameter, pitch length, and array configuration. Also, other absorption boosting techniques such as using aluminum gallium arsenide (AlGaAs) as a passivation material and coating a silicon dioxide (SiO<sub>2</sub>) shell on GaAsSb nanowires were employed. Results show that nanowires that have a diameter that range from 100 nm -150 nm with a pitch length of 400 nm provide the optimal absorbance spectra according to simulations for both the axial and core-shell configurations. Also including a SiO<sub>2</sub> shell to the axial nanowire was found to boost absorption in the near infrared region by approximately 30 %. Results show that Lumerical FDTD can be used as a powerful simulation tool for optical simulation of nanowire arrays for device application while reducing experimental iterations.

## Greener synthesis of high aspect ratio copper oxide nanowires for potential applications

Gayani Pathiraja, Hemali Rathnayake

Controlled synthesis of one-dimensional nanostructures such as nanowires are most fascinating for wide range applications due to their superior performances based on quantum confinement effects. Here, we demonstrate a novel facile and greener synthesis method to fabricate high aspect ratio of one-dimensional CuO nanowires from directed self-assembly of Cu(OH)<sub>2</sub> nanocrystals guided by the oriented attachment mechanism via post-annealing. This surfactant free, one-pot sol-gel route at low temperature allows us to make higher aspect ratio of CuO nanowires with controlled-dimensions over a large area. The respective Raman, XRD and XPS spectroscopies confirm the chemical composition of CuO nanowires and their purity. The synthesized CuO nanowires has average diameter of  $26.5 \pm 2.4$  nm and aspect ratio of  $280.9 \pm 18.0$ . Further, the analysis of electrochemical properties of synthesized CuO nanowires have shown the suitability for potential electrochemical applications of capacitors and energy storage devices.

## Pitch-Dependent Study of Patterned GaAsSbN Nanowires using Boltzmann Sigmoidal Model

Sean Johnson, Rabin Pokharel, Michael Lowe, Hirandeep Kuchoor, Surya Nalamati, and Shanthi Iyer

This study presents the application of the Boltzmann sigmoidal model on patterned nanowires (NWs) of dilute nitride GaAsSbN on Si (111) silicon substrates by self-catalyzed plasma-assisted molecular beam epitaxy. Patterned NW array with GaAsSb of Sb composition of 3% as a stem provided the best yield of vertical NWs. Large bandgap tuning of  $\sim 90$  meV, as ascertained from 4K photoluminescence (PL), over a pitch length variation of 200 nm to 1000 nm has been demonstrated. Pitch-dependent axial and radial growth rates reveal a logistic sigmoidal growth trend that differs from those commonly observed in other patterned non-nitride III-V NWs. Sigmoidal fitting provides further insight into the PL spectral shift arising from differences in Sb and N incorporation from pitch induced variation in secondary fluxes. Results show that sigmoidal fitting can be an effective tool for designing patterned NW arrays of optimal pitch length for dilute nitrides, and other highly mismatched alloys and heterostructures.



## Pitch-Dependent Study of Patterned GaAsSbN Nanowires using Boltzmann Sigmoidal Model

Sean Johnson, Rabin Pokharel, Michael Lowe, Hirandeep Kuchoor, Surya Nalamati, and Shanthi Iyer

This study presents the application of the Boltzmann sigmoidal model on patterned nanowires (NWs) of dilute nitride GaAsSbN on Si (111) silicon substrates by self-catalyzed plasma-assisted molecular beam epitaxy. Patterned NW array with GaAsSb of Sb composition of 3% as a stem provided the best yield of vertical NWs. Large bandgap tuning of  $\sim 90$  meV, as ascertained from 4K photoluminescence (PL), over a pitch length variation of 200 nm to 1000 nm has been demonstrated. Pitch-dependent axial and radial growth rates reveal a logistic sigmoidal growth trend that differs from those commonly observed in other patterned non-nitride III-V NWs. Sigmoidal fitting provides further insight into the PL spectral shift arising from differences in Sb and N incorporation from pitch induced variation in secondary fluxes. Results show that sigmoidal fitting can be an effective tool for designing patterned NW arrays of optimal pitch length for dilute nitrides, and other highly mismatched alloys and heterostructures.

## Growth cobalt oxide nanograin on aligned electrospun N-doped nanofiber for electrochemical detection of dopamine secreted by living cells

Ziyu Yin, Jianjun Wei

With the more desirable for biological molecule detection in the early clinic diagnosis, such as dopamine secreting by living cells, a flexible miniaturized electrochemical biosensor with high sensitivity, wide workable detection range is demanding. Dopamine (DA) is a significant neurotransmitter, associated with regulating neuronal signal transduction and several critical illnesses, such as Parkinson's diseases and schizophrenia. Therefore, the accurate detection DA levels provides an early diagnosis and a tool to follow up the output of the treatments. In this work, a new hybrid flexible electrochemical sensor has been created by decorating closely packed cobalt oxide (Co<sub>3</sub>O<sub>4</sub>) nanograins on electrospun nitrogen doped carbon nanofibers (ENCNFs), where the Co<sub>3</sub>O<sub>4</sub> nanograins uniformly distributing on the surface of ENCNFs is maximized. The hypothesis of the work is by using integrated Co<sub>3</sub>O<sub>4</sub> nanograins on the carbon nanostructured materials (ENCNFs), the synergetic of their promising potential could be taken to the performance and characteristics of the electrochemical biosensors and achieve a completely new level. In addition, the real-time detection of DA released from pheochromocytoma (PC 12) cells by highly concentrated K<sup>+</sup> stimulation is recorded by this flexible sensor, enabling the novel sensor to provide a facile application in early clinic diagnosis.

## Bio-inspired Soft Multi-scale Capacitive Stress Sensor based on dual structure Liquid Metal Elastomer Foam

Jiayi Yang, Ki Yoon Kwon, Shreyas Kanetkar, Michael D. Dickey.

**Background:** Capacitive stress sensors have attracted significant interest due to their high sensitivity and low energy consumption and have been used in a variety of applications, including healthcare monitoring[1], human-machine interfaces[2], and electronic textiles[3]. Capacitive stress sensors consist of a dielectric layer sandwiched between electrodes. Sensitivity and measurement range of capacitive sensors can be increased by decreasing or increasing the elastic modulus of the dielectric layer, which leads to a contradiction with each other. To solve this problem, a capacitive stress sensor based on dual-structure liquid metal elastomer foam (DSLMEF) is proposed. Inclusion of liquid metal in elastomer is used to tune the dielectric constant of the mixed material[4], which was shown to give the higher stress sensitivity[4].

**Results:** The DSLMEF is composed of a stiff elastomer slab (elastic modulus:  $\sim 655$  kPa) and a soft liquid metal elastomer foam (LMEF, elastic modulus:  $\sim 7$  kPa). Small stress ( $< 10$  kPa) only deforms the soft LMEF, and large stress ( $> 10$  kPa) deforms the soft LMEF and the stiff elastomer slab at the same time. Using the DSLMEF as the dielectric layer, a capacitive stress sensor with high sensitivity ( $0.073$  kPa $^{-1}$ ), and large stress measurement range ( $200$  kPa) is demonstrated.

**Conclusions:** We report a bioinspired soft multi-scale capacitive stress sensor based on dual structure liquid metal elastomer foam. The fabrication process of the sensor is easy to implement, low cost, and environment friendly. Compared with other capacitive soft stress sensors, this work achieves a better combination of sensitivity and measurement range. In addition, the high elastic modulus and high energy loss coefficient of DSLMEF also mimic the dermis of human skin, which can cushion objects from stress and strain. The development of the bioinspired soft multi-scale capacitive stress sensor based on DSLMEF has important scientific value and practical significance.

### References:

1. Gao, Y.; Yu, L.; Yeo, J. C.; Lim, C. T. Flexible Hybrid Sensors for Health Monitoring: Materials and Mechanisms to Render Wearability. *Adv. Mater.* 2020, 32 (15), e1902133, DOI: 10.1002/adma.201902133.
2. Hammock, M. L.; Chortos, A.; Tee, B. C.; Tok, J. B.; Bao, Z. 25th anniversary article: The evolution of electronic skin (e-skin): a brief history, design considerations, and recent progress. *Adv. Mater.* 2013, 25 (42), 5997-6038, DOI: 10.1002/adma.201302240.
3. Kim, D. C.; Shim, H. J.; Lee, W.; Koo, J. H.; Kim, D. H. Material-Based Approaches for the Fabrication of Stretchable Electronics. *Adv. Mater.* 2020, 32 (15), e1902743, DOI: 10.1002/adma.201902743.

4. Yang, J. Y.; Tang, D.; Ao, J. P.; Ghosh, T.; Neumann, T. V.; Zhang, D. G.; Piskarev, E.; Yu, T. T.; Truong, V. K.; Xie, K.; Lai, Y. C.; Li, Y.; Dickey, M. D. Ultrasoft Liquid Metal Elastomer Foams with Positive and Negative Piezopermittivity for Tactile Sensing. *Adv. Funct. Mater.* 2020, DOI: ARTN 2002611

10.1002/adfm.202002611.

## Porous liquid infused surfaces in microfluidics for fluid delivery: Pressure and heat transfer measurements

Reginald Goodwin, Bolaji Sadiku, Jeffrey Alston

Applying the effects of non-wetting surface chemistry and exploiting “The Lotus Effect” are practices common to the art of creating liquid repellant surfaces. The Lotus leaf illustrates water repellency and is an example of water repellency (hydrophobicity). This is functionalized by the nanostructures once unknown. Micro and Nanotexturing techniques also accompany the process of creating superhydrophobicity and superoleophobicity. There is, however, another method of surface functionalization from nature that we can exploit in the laboratory, Slippery Liquid-Infused Porous Surfaces (SLIPS). SLIPS are biomimetic surfaces inspired by the Nepenthes pitcher plant that are textured surfaces infused with liquids allowing the study of low-adhesion interfaces of sessile droplets for zero contact angle hysteresis and flowing fluids. SLIPS has applications in Microfluidics, Nanofluidics, hydrophobicity, and ice nucleation inhibition. This study fabricates SLIPS surfaces on porous glass using a commercial chemical etchant on glass slide substrates. An infused porous glass with a perfluoropolyether liquid, which is immiscible with both oil and water. The product is a self-healing surface that affects both pressure and heat transfer in microfluidic devices. This study evaluates an experimental matrix of porous glass fabrication parameters and assesses microfluidic-SLIPS for their effect on backpressure and heat transfer in microscale fluid delivery devices.

## Characterizing the properties of GaN- microorganism biointerfaces

Alexey Gulyuk, Dennis LaJeunesse, Ramon Collazo, Albena Ivanisevic

Possessing many unique properties, semiconducting materials have been extensively utilized in biocomputing, bioengineering and in healthcare. Biointerfaces based on inorganic semiconducting materials introduce unconventional paths for bioinformatics and biosensing. Thus, understanding how the properties of a semiconducting substrate may influence the behavior and properties of biofilms formed on their surfaces, one may develop programmable biointerfaces with desired characteristics.

In this study, it was proven that UV light exposure can alter the interfacial properties of variably doped GaN substrates. First, the GaN substrates were characterized by Atomic Force Microscopy, Kelvin Probe Force Microscopy and X-ray Photoelectron Spectroscopy. Next, the GaN-*Pseudomonas aeruginosa* biointerfaces were examined for possible responses. These responses were detected by analyzing intracellular  $\text{Ca}^{2+}$  concentrations, catalase activity, and reactive oxygen species concentrations. Furthermore, GaN-*Saccharomyces cerevisiae* biointerfaces were examined for possible stress-response by increasing amounts of intracellular reactive oxygen species.

Performed analysis supports the idea that alterations in external conditions can change substrate properties that will further influence characteristics of an entire biointerfacial structure. Particularly, *P. aeruginosa* and *S. cerevisiae* biofilms can be controlled by the properties of the GaN substrates and the amount of contact time.

## Diffracted Disk Registration and Lattice Fitting for Convergent-Beam Electron Diffraction Patterns

Sihan Wang, Tim Eldred, Jacob Smith, Wenpei Gao

An automated processing of diffracted disk registration and lattice parameter extraction is presented on convergent-beam electron diffraction patterns with an accuracy of sub-picometer scale. The method includes a cross-correlated pattern with a blob detection, followed by a refinement step to locate all the detectable disks, and then a lattice fitting algorithm is applied to optimize and output two lattice vectors in each pattern. The results on both simulated patterns and experimental patterns show a decent robustness of our method on noisy patterns and challenging real cases. We also demonstrate a strain mapping of Pd@Pt nanoparticles as one of the applications. With high accuracy and noise robustness, our method is promising for further structural analysis and has a potential to be employed on other applications such as orientation, charge and symmetry mappings.



## Sponsors

